Evaluation of Microstructure and Tribological Properties of GX120Mn13 and GX120MnCr18-2 Cast Steels

B. Kalandyk [a, *], R. Zapała [a], J. Kasińska [b], M. Madej [b]

[a] AGH University of Science and Technology, Department of Cast Alloys and Composites Engineering,
Faculty of Foundry Engineering, ul. Reymonta 23, 30-059 Krakow, Poland
[b] Kielce University of Technology,
al. Tysiąclecia Państwa Polskiego 7, 25-314 Kielce, Poland
* Corresponding author. E-mail address: bk@agh.edu.pl

Abstract

The results of microstructure examinations and hardness measurements carried out on two selected grades of high-manganese cast steel with an austenitic matrix, i.e. GX120Mn13 and GX120MnCr18-2, are presented. The examinations of the cast steel microstructure have revealed that the matrix of the GX120MnCr18-2 cast steel contains the precipitates of complex carbides enriched in Cr and Mn with two different morphologies. The presence of these precipitates leads to an increase in hardness by approx. 30 HB compared to the GX120Mn13 cast steel. Samples cut out from the tested materials were loaded (10 strokes) with an energy of 53 J, and then a ball-on-disc tribological test was performed. The test was carried out in reciprocating motion under technically dry friction conditions. While analyzing the obtained results of the microstructure, hardness, and abrasion tests, it was found that the presence of the hard carbide precipitates in the plastic matrix of the tested GX120MnCr18-2 cast steel promoted an increase in hardness, but also led to chipping of these particles from the alloy matrix, thus contributing to micro-cutting during friction.

Keywords: High manganese cast steel, Microstructure, Hardness, Wear resistance

1. Introduction

Austenitic, high-manganese (approx. 12% - 14% Mn) steels (also known as Mangalloy) and cast steels are characterized by very high mechanical properties, i.e. YS = 375 MPa, UTS = 965 MPa, A = 50%, RA = 40%, Charpy V-notch impact strength = 169 J at ambient temperature and 7 J at -196°C, as-quenched hardness = 190 HB and approx. 500 HB in solution-treated state after hardening [1-3]. These high mechanical properties are accompanied by exceptionally good abrasion resistance under operating conditions with high dynamic loads or shock wave

hardening [3-8]. This effect is referred to as "self-hardening" by cold work (self-strengthening of austenite). A combination of these properties has resulted in the fact that components made from high-manganese steel and cast steel find application, among others, for railroad frogs, grinding mill lines, impact hammers, oil well drilling equipment, woodworking tools, crushers in the car recycling industry, and for various military applications [5-11]. Another important property of high-manganese steels is their paramagnetism used in railway communication systems (fast levitation railways), submarines, nuclear reactors, or nonmagnetic plater for electromagnets [7, 8]. The deep drawing technology developed in the 1990s allowed for the production of armour

plates and military helmets competing with titanium alloys, among others in price [8]. In recent years, research has been conducted on explosive welding of bimetallic sheets using Hadfield steel [12]. Owing to the fact that high strength properties are well preserved also at sub-zero temperatures (even down to -196°C), high-manganese steels and cast steels have found application in cryogenics [6, 13]. In this area of application, high-manganese steels and cast steels containing >15% Mn have been developed. They are characterized by low magnetic permeability and good strength at low temperatures, which allows these materials to be used in modern transport systems, liquefied gas storage and transport structures, and in studies of nuclear fusion [7]. In recent years, many modifications of the basic chemical composition of the GX120Mn13 cast steel have been developed, mainly by introducing carbide-forming elements such as Cr, Ni, Mo, Ti, V or Bi [5, 8, 11, 14], the presence of which in the microstructure is to increase strength and plasticity, and thus extend the scope of application of this cast steel by improving its wear resistance under conditions of low impact loads [15, 16]. The presence of Mo (2-3%) in these materials increases both resistance and plasticity. The addition of Cr (approx. 2%) contributes to an increase in hardness and slightly reduces plasticity in castings with a small wall thickness. The introduction of Ni (up to approx. 4%) reduces the cooling rate, stabilizes austenite, inhibits nucleation of acicular carbides, increases plasticity, but reduces abrasion resistance. However, Fedorko et al. [5] in their research on railway turnout castings, applying the recommended railway impact test, have found a negative effect of both Cr and Ni on impact toughness. On the other hand, the addition of Ti and Zr leads to the formation of nitrides in the matrix with reduction in ductility. Another frequently added element is V. After introducing 0.5-2% V, an increase in the yield point is observed through the formation of stable carbonitrides [15-18], the size and distribution of which affect the mechanical properties and wear resistance while reducing the impact energy [19]. It should be remembered, however, that in the case of these alloys, it is the content of C and Mn that has a decisive influence on their properties [9, 20].

Hardening the surface layer of high-manganese steel and cast steel components guarantees high abrasion resistance under operating conditions. If the operating stress is too low, sufficient hardening may not occur, and then the abrasion resistance of this cast steel will not differ from that of common carbon cast steel. Numerous research works have been devoted to the hardening mechanism itself, but so far there is no single theory explaining the hardening mechanism of this unique material. There are, however, two theories assuming that [6, 8, 16, 21-23]:

– hardening has its origin in the stabilization of manganese austenite during deformation and changes occurring in the surface and subsurface layers, including the reconstruction of a dislocation structure, the formation of stacking faults, and the occurrence of twins and slip lines,

– hardening is associated with the loss of austenite stability and the occurrence of phase transformations as a result of

which ε, α martensite is formed; additionally there is also segregation of C and its precipitates at dislocations.

Polish foundries produce castings from the common GX120Mn13 steel, used mainly for railway turnouts, and from the GX120MnCr18-2 steel for elements of crushers used in the mineral and mining industries.

2. Materials and Experimental Methods

Tests were carried out on samples with dimensions of 90x22x15 mm made from the high-manganese GX120Mn13 and GX120MnCr18-2 cast steels. Both grades were melted under industrial conditions. Table 1 gives their chemical composition. The tested materials were subjected to a heat treatment typical for these grades of cast steel, i.e. solution treatment at a temperature of 1080°C. Under laboratory conditions, the samples were subjected to impact loading with an energy of 53J performed in a series of ten strokes. The loading diagram is shown in Figure 1.
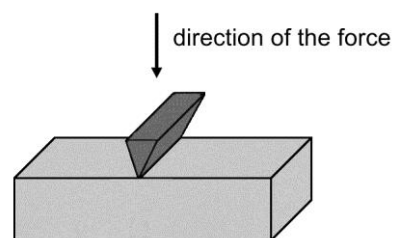

Fig. 1. Schematic diagram of the sample loading system

The hardness of the tested materials was measured using Brinell hardness tester provided with a D = 2.5 mm diameter steel ball. In selected areas of the microstructure, hardness was measured by Vickers method using Hanemann VEBC microhardness tester operating under a load of 0.9807 N (0.1 kG). The Leica MEF4M light microscope, the JSM 7100F field emission scanning electron microscope and an EDS analyzer were used to study the microstructure. Metallographic tests were carried out on samples after nital etching. The abrasion resistance tests were carried out at room temperature on the TRB3 tester. The device was operating in a flat disc (tested material) - counter-sample (a 6 mm diameter SiC ball) system. The tests were carried out in dry condition applying the following parameters: a load of 10N, max. amplitude of 6 mm and max. speed of 0.02 m/s. The wear resistance tests were carried out on a surface perpendicular to the load applied in two areas of the sample, i.e. in the area directly adjacent to the surface to which the load was applied and at a distance of approx. 5 mm from the load applied.

Table 1.
Chemical composition of the investigated cast steels

Designation	C	Mn	P	S	Si	Cr	Mo	Ni	Al
	wt %								
GX120Mn13	1.27	11.80	0.047	0.011	0.70	-	0.06	0.04	0.042
GX120MnCr18-2	1.29	18.04	0.054	0.007	0.50	2.30	0.15	0.11	0.039

3. Results and Discussion

3.1. Microstructure

The microstructures of GX120Mn13 and GX120MnCr18-2 cast steels subjected to solution treatment at 1080°C are shown in Figures 2 and 3, respectively. The application of this heat treatment eliminates from the cast steel matrix, composed of manganese austenite, the precipitates of carbide $(Fe,Mn)_3C$ and phosphorus eutectic, so characteristic of the high-manganese steel and cast steel [24]. In the case of the GX120MnCr18-2 cast steel containing the addition of approx. 2% of the carbide-forming Cr, the microstructure contains complex Cr and Mn carbides with different morphology, i.e. fine and/or more compact (Fig. 3). The results of the chemical analysis of the carbide precipitates and the matrix of both alloys are shown in Table 2, 3, and Figs. 4, 5.
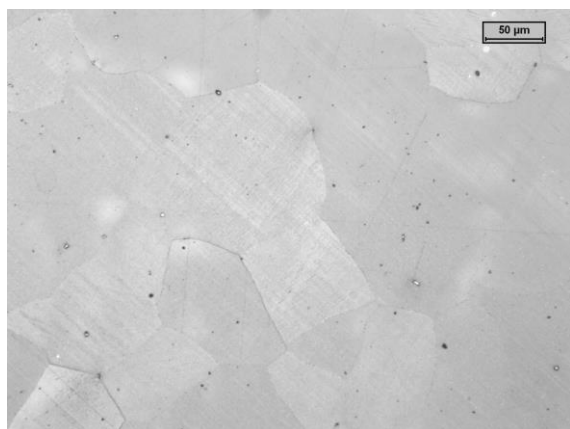

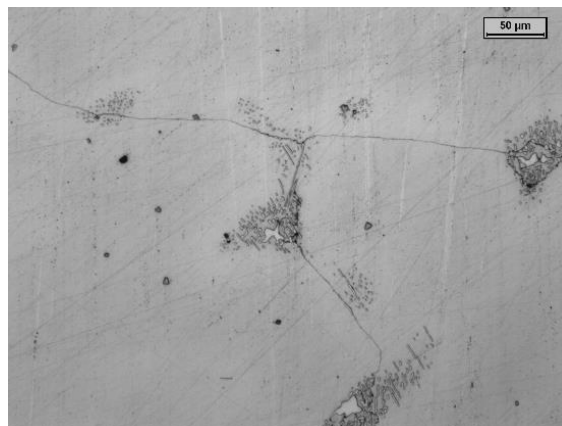Fig. 3. Microstructure of the GX120MnCr18-2 cast steel, light microscope, nital etching

Fig. 2. Microstructure of the GX120Mn13 cast steel, light microscope, nital etching
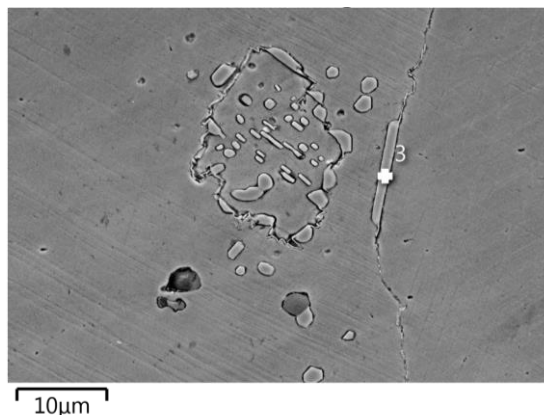

Fig. 4. Example of the area selected for fine carbide analysis in GX120MnCr18-2
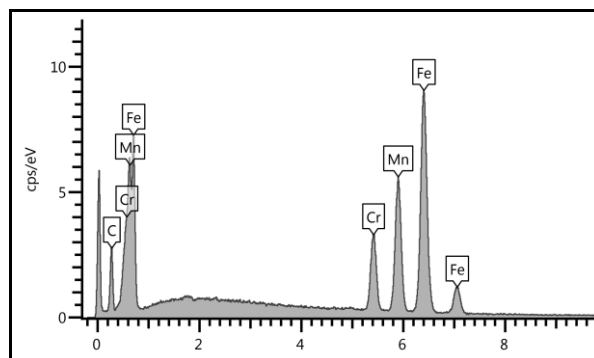

Fig. 5. Sample X-ray spectrum of point 3 in Figure 4

Table 2.
Chemical analysis of precipitates present in the GX120MnCr18-2 cast steel

Area of analysis	Si	Mn	Cr	Fe
	wt %			
Large precipitates	-	25.1	10.8	53.7
Fine precipitates	0.2	23.6	8.4	56.6

The SEM-EDS studies have shown that in both carbide morphologies the content of Mn ranges from 23.6 to 25%, and that of Cr from 8.4 to 10.8%. The presence of complex carbides enriched in Mn and Cr reduced the Mn content in the matrix to a level of approx. 16.8%, which is consistent with literature reports and is associated with the phenomenon of segregation favouring Mn changes in the matrix [7]. The GX120Mn13 cast steel matrix contains, on average, about 10.8% Mn, which means that the matrix of the GX120MnCr18-2 cast steel contains about 6% more Mn than the investigated GX120Mn13 cast steel (Table 3).

Table 3.
Chemical analysis of austenitic matrix present in the tested cast steel-grades

Area of analysis	Si	Mn	Cr	Fe
	wt %			
Austenite in GX120Mn13 cast steel	0.7	10.8	-	rest
Austenite in GX120MnCr18-2 cast steel	0.5	16.8	1.9	rest

3.2 Changes in microstructure as a result of loading

Visual assessment of changes that occurred in the tested materials as a result of the applied load has revealed the formation of a deformation (cavity) in the surface layer of the material, while a characteristic "protrusion" was observed on the side surface (Fig. 6) extending into the material to a depth of approx. 5 mm for the GX120Mn13 cast steel (Fig. 2) and approx. 2.5 mm for the GX120MnCr18-2 cast steel (Fig. 3).
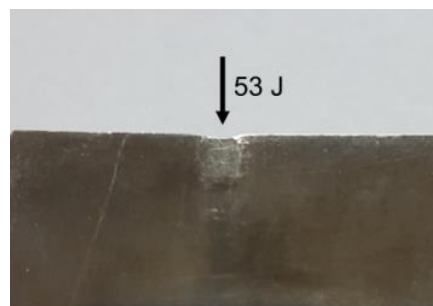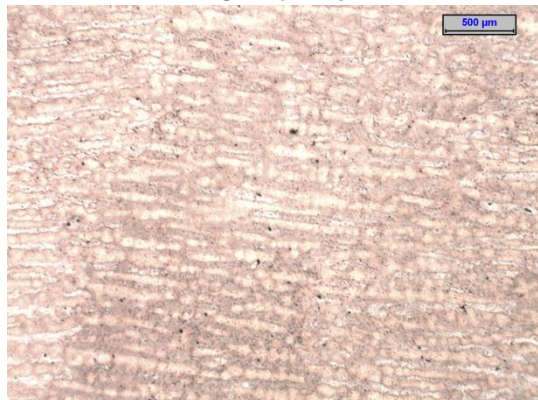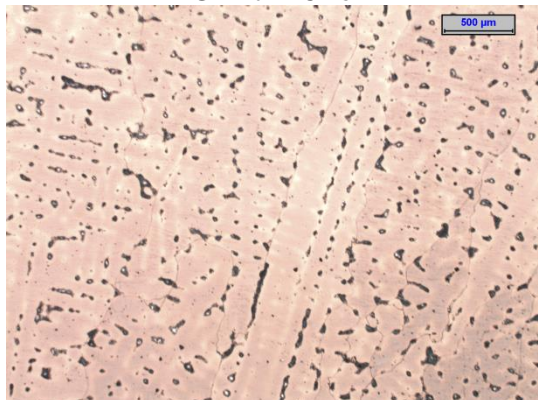

Fig. 6. View of the GX120Mn13 cast steel sample after loading

Hence, in the further part of the research, examinations of the microstructure of the GX120Mn13 and GX120MnCr18-2 cast steels covered areas located on the surface perpendicular to the applied load. The changes that took place in the microstructure of both tested materials are shown in Figures 7 and 8.
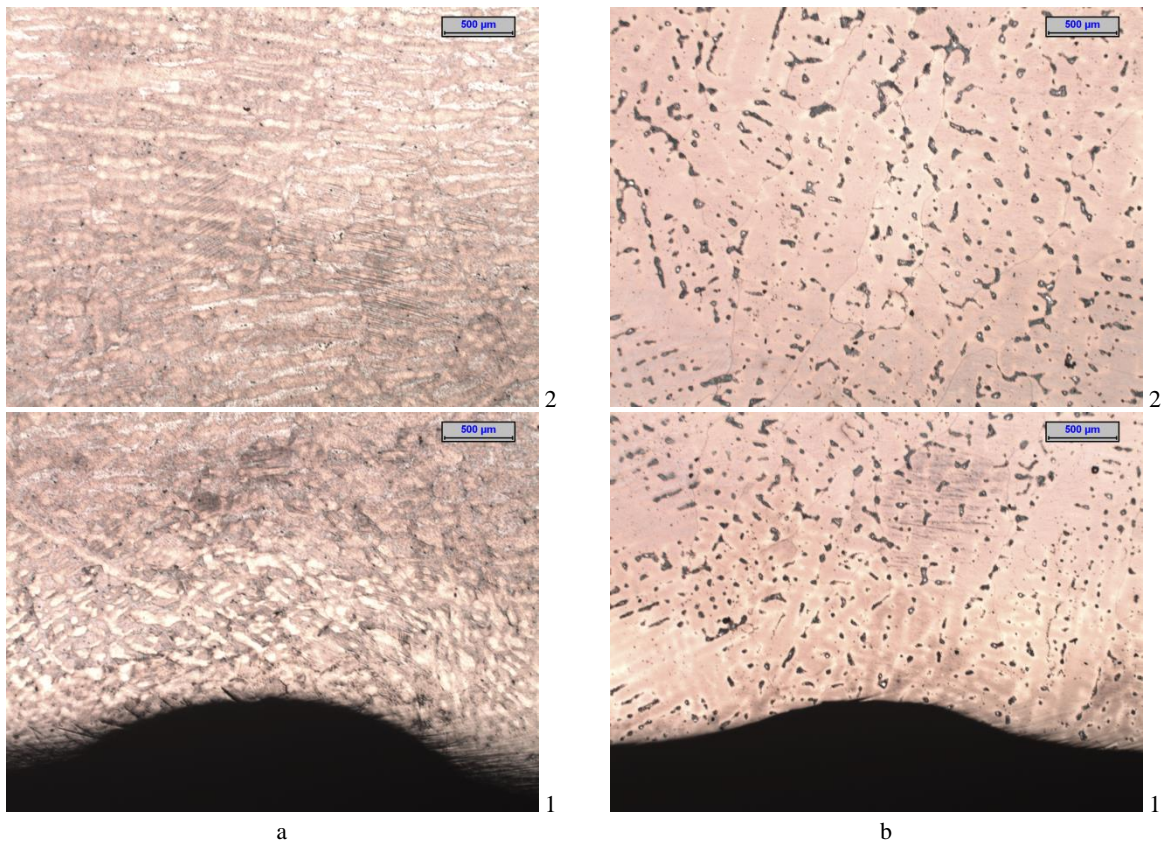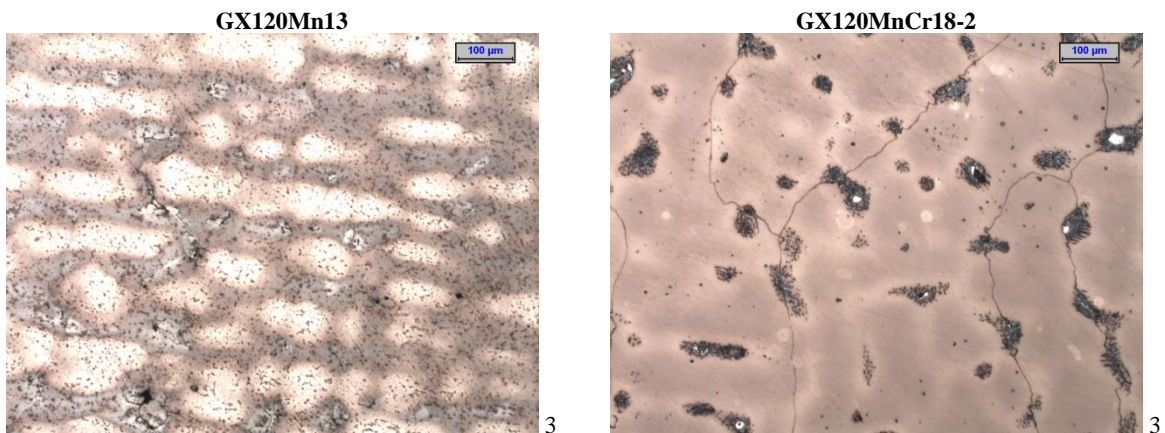
GX120Mn13

GX120MnCr18-2

Fig. 7. Cast steel microstructure in the area of load application, 1-3 areas penetrating deep into the material as a result of impact loads - 25x; light microscope, nital etching
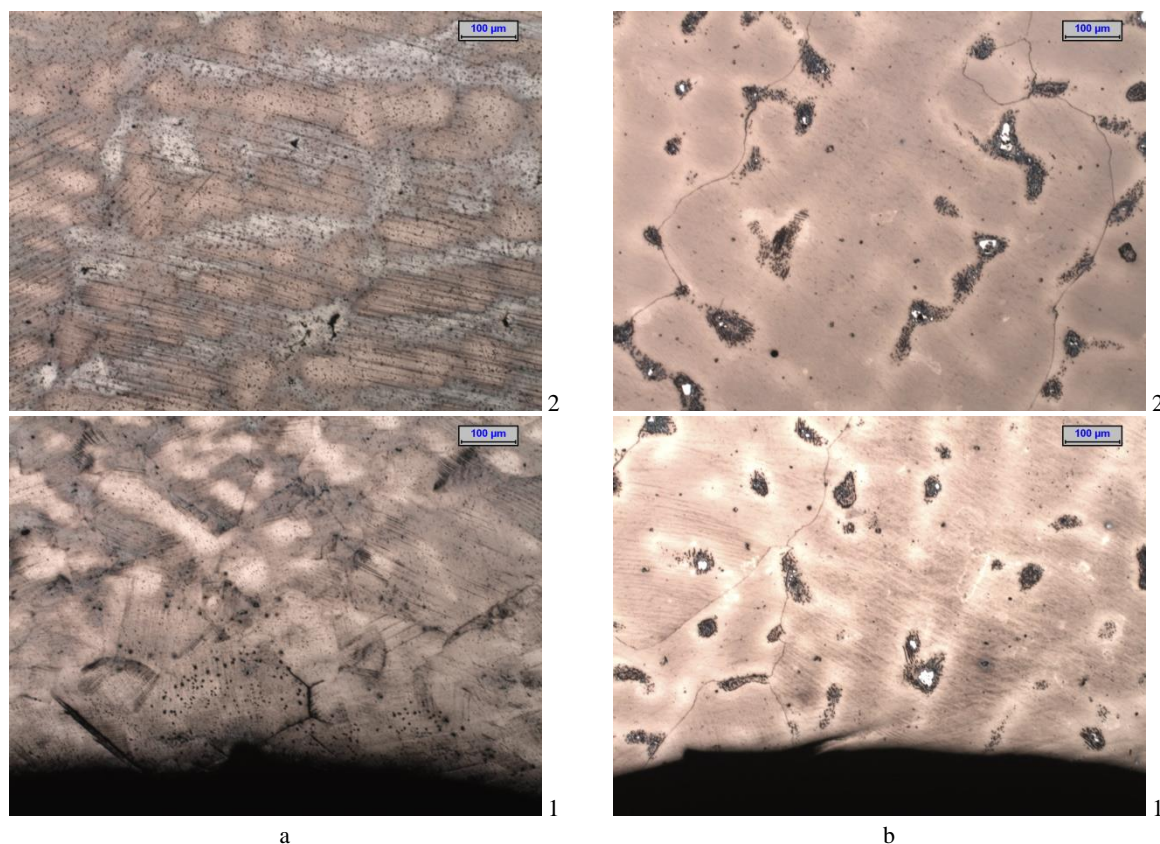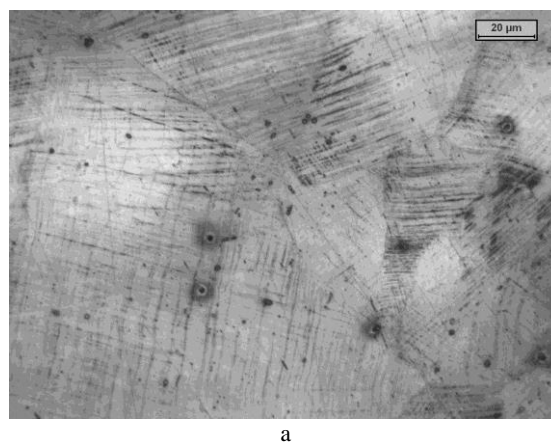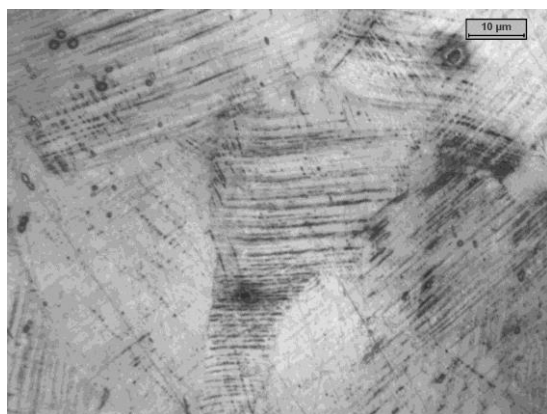
GX120Mn13

GX120MnCr18-2

Fig. 8. Cast steel microstructure in the area of load impact from three zones; 100x; light microscope, nital etching

What makes the microstructures of both materials essentially different from each other is the presence in the GX120Mn13 cast steel, in the area of the direct impact of the applied load, of a zone surrounding the place of impact, differing from the rest of the microstructure and having a thickness of approx. 700 μm (Fig. 7a – zone 1). In the GX120MnCr18-2 cast steel, on the contrary, no significant differences in the microstructure were found when moving away from the place of the impact load application into the material (zones 1 - 3). The precipitates of complex carbides enriched in Mn and Cr, characteristic for this cast steel, occurred both on the boundaries and inside the grains and were evenly distributed throughout the microstructure, regardless of the load interaction zone (Figs. 7 and 8).

The analysis of the GX120Mn13 cast steel microstructure has additionally revealed the presence of a crack in zone 1 running along the grain boundary from the surface layer (Fig. 8a), probably initiated by the undissolved precipitates of manganese cementite. In zones 1 and 2, the presence of lines (bands composed of short lines) indicating activation of the slip systems was observed (Fig. 9). The analysis of microhardness measurements in the area of line compaction visible in the microstructure of both materials (e.g. Fig. 9) has shown the increase in hardness to 369 HV0.1 for the GX120Mn13 cast steel (matrix microhardness of 285 HV0.1) and to 504 HV0.1 for the GX120MnCr18-2 cast steel (matrix microhardness of 463 HV0.1). The comparison of the changes that took place in the microstructure and microhardness of both materials within the

area of the applied load clearly shows that the observed differences result from the increased concentration of Mn in austenite and from the presence of complex carbide precipitates in the microstructure of the GX120MnCr18-2 cast steel.
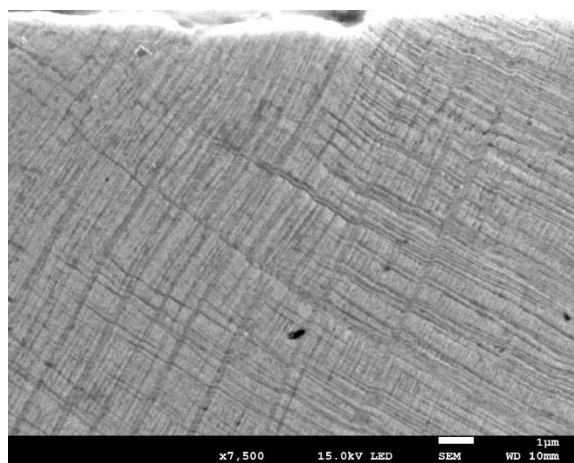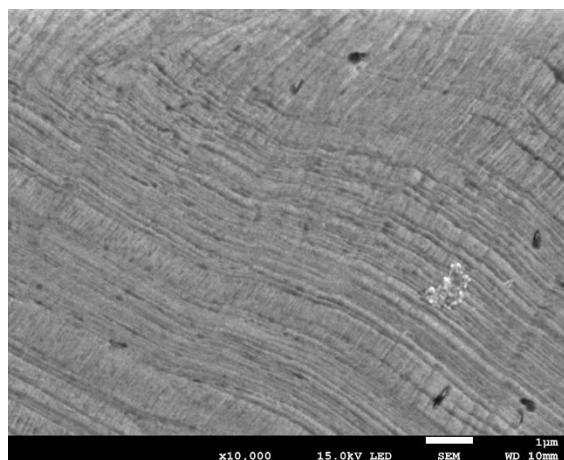

a

Fig. 9. The microstructure of GX120Mn13 cast steel in zone 2; light microscope, nital etching

Figures 10a and 10b show the microstructure of the GX120Mn13 cast steel after deformation. In both drawings, the slip lines originating from two different slip systems are visible. As a result of deformation, in the following sequential slip systems, characteristic faults can be observed (more visible in Fig. 10a). They are caused by the intersection of the first (primary) slip system and the second (secondary) slip system. Further plastic deformation in the secondary slip system leads to the formation of "deflections" in the primary slip lines (more visible in Figure 10b).

Fig. 10. Examples of the microstructure of GX120Mn13 cast steel in zone 1 - directly adjacent to the area of load application; 7500x (a), 10 000x (b); scanning microscope

3.3. Changes in hardness as a result of load application

The increased content of Mn and the addition of Cr in the GX120MnCr18-2 cast steel, compared to the GX120Mn13 cast steel, increased the initial hardness from 213 HB for the GX120Mn13 cast steel to 242 HB for the GX120MnCr18-2 cast steel. As a result of the applied impact load, the hardness in the near-surface area of the GX120Mn13 cast steel increased to approx. 260 HB, i.e. by approx. 32%, while for the GX120MnCr18-2 cast steel this increase amounted to 278 HB, i.e. by approx. 13%. At a distance of 8 mm from the applied load, the hardness of the GX120Mn13 cast steel decreased to about 220 HB, while remaining practically unchanged for the GX120MnCr18-2 cast steel. Only at a distance of approx. 16 mm, the hardness of the GX120MnCr18-2 cast steel decreased by approx. 10 HB. In turn, the hardness of the GX120Mn13 cast steel was the same as at a distance of 8 mm, thus indicating some stabilization of the hardness results. The obtained results showed the tendency of the GX120Mn13 cast steel hardness values to decrease with the growing distance from the applied load. A similar result was obtained in [25]. In the case of the GX120MnCr18-2 cast steel, no such clear tendency was found, and hardness values remained at a comparable level. Therefore microhardness measurements were carried out. The measurements covered the range reaching into the material to a distance of 5 mm. The obtained results are shown in Figures 11 and 12.
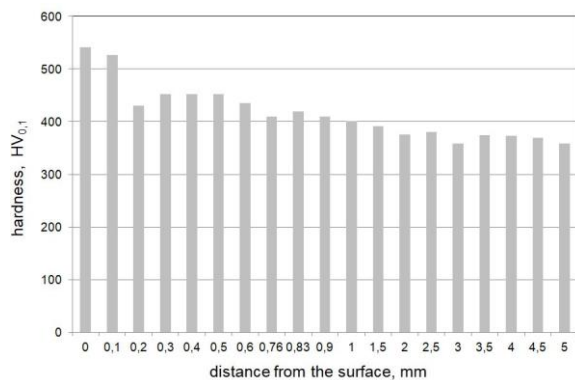
Fig. 11. Hardness changing in the tested GX120Mn13 cast steel from the surface to a depth of 5 mm

In the GX120Mn13 cast steel, high microhardness was obtained in the near-surface areas, but a noticeable decrease was observed when moving deeper into the material. On the other hand, in the case of the GX120MnCr18-2 cast steel, no significant differences in microhardness were observed in the tested section.
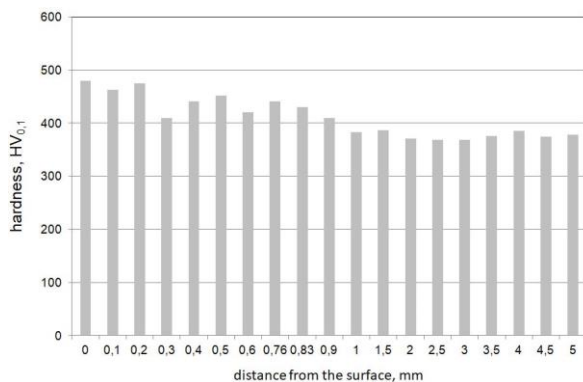
Table 4.
Tribological characteristics and wear indicators of the tested materials

Cast steels	GX120Mn13	GX120MnCr18-2
hardened area		
Average max. wear depth * [μm]	3.098	4.097
Average wear surface area * [μm²]	189.8	91.06
Average coefficient of friction	0.43	0.64
area 5mm distant from the surface		
Average max. wear depth * [μm]	1.936	3.500
Average wear surface area * [μm²]	250.7	552.7
Average coefficient of friction	0.51	0.34

* the average maximum wear depth on the cross-section and the average wear surface area were determined based on 100 profiles

Fig. 12. Hardness changing in the tested G120MnCr18-2 cast steel from the surface to a depth of 5 mm

3.4 Abrasive wear tests

The results of tribological tests carried out on the investigated cast steels are presented in Table 4 and shown for the GX120Mn13 cast steel in Figure 13 and for the GX120MnCr18-2 cast steel in Figure 14. As expected, for both materials, the average wear surface area was smaller at the hardened surface than at a distance of 5 mm from this surface. Definitely smaller wear areas were obtained in the hardened area of the GX120MnCr18-2 cast steel, which was accompanied by the greatest depth of wear, probably caused by chipping of Mn- and Cr-containing carbides, distributed in the microstructure, during the test. Loose particles of carbides could additionally contribute to the intensification of micro-cutting, as shown by the surface topography of the GX120MnCr18-2 cast steel (Fig. 14). Consequently, it might lead to increased abrasion through mechanical or abrasive-mechanical modes of wear.

a

b

Fig. 13. View of the topography of the GX120Mn13 cast steel surface after the test - hardened at the surface (a) and at a distance of 5 mm from the surface (b)
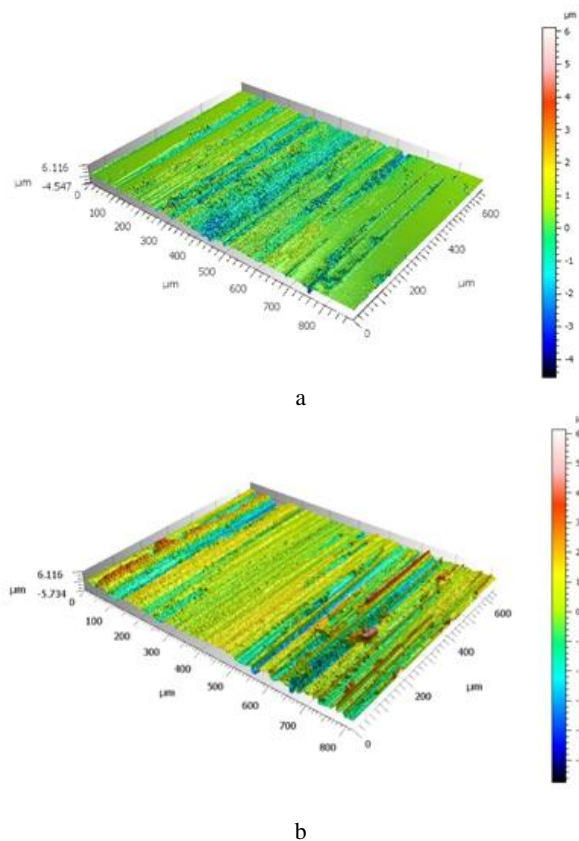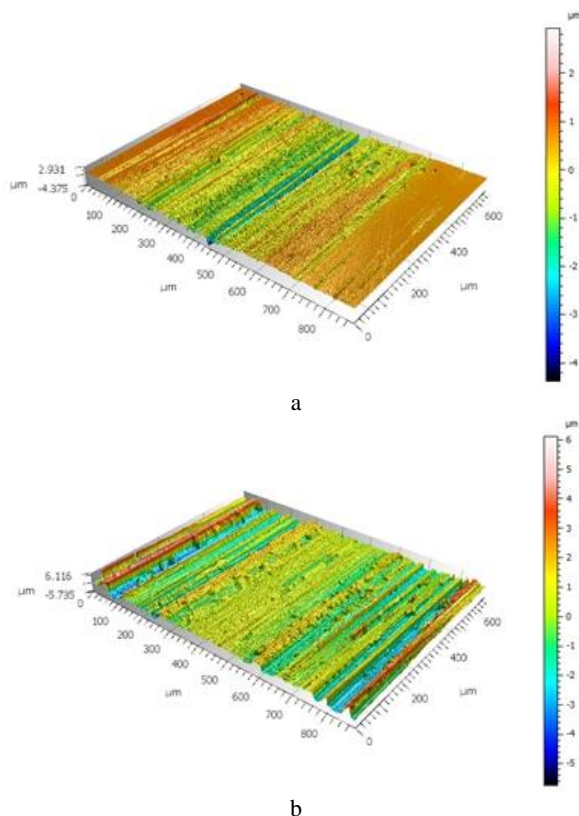
a

b

Fig. 14. View of the topography of the GX120MnCr18-2 cast steel surface after the test - hardened at the surface (a) and at a distance of 5 mm from the surface (b)

4. Conclusions

The matrix of the tested cast steel grades was composed of manganese austenite with an average Mn content of 10.8% Mn for the GX120Mn13 cast steel and approx. 16.8% Mn for the GX120MNCr18-2 cast steel. The higher Mn content and the addition of Cr caused an increase in the hardness of the GX120MNCr18-2 cast steel by approx. 30 HB as compared to the GX120Mn13 grade.

In both tested materials, compared to the initial state, hardness was found to increase as a result of the applied load. The strengthening of both materials, measured in the near-surface areas and expressed in the HB hardness units, increased by approx. 32% and 13% for the GX120Mn13 cast steel and the GX120MNCr18-2 cast steel, respectively. The main reason for the increase in the hardness of the GX120Mn13 cast steel was strengthening by the slip mechanism.

The average wear surface area in the hardened zone was two times smaller for the GX120MnCr18-2 cast steel than for the GX120Mn13 cast steel and was accompanied by a greater average maximum depth of wear. Compared to the hardened area, in the non-hardened zone, the average wear surface area increased for both materials. The obtained results have shown that the average wear surface area and the maximum wear depth assumed much higher values for the GX120MnCr18-2 cast steel compared to the GX120Mn13 cast steel.

5. References

[1]   Standard PN-EN 10349: 2009. Steel castings - Austenitic manganese steel castings.

[2]   Banerjee, M.K. (2017). Heat Treatment of Commercial Steels for Engineering Applications. *Comprehensive Materials Finishing*. 2, 180-213.

[3]   Dobrzański, L.A. (2002). *Fundamentals of materials science and metal science*. Warszawa: Wyd. Naukowo-Techniczne. ISBN: 83-204-2793-2. (in Polish).

[4]   Baza materiałowa. Total materia. (June 2021). Retrieved August 13, 2021, from https://portal-1totalmateria1com 1000022kc0110.wbg2.bg.agh.edu.pl/search/quick/materials/1 040932/material-description.

[5]   Fedorko, G., Molnár, V., Pribulová, A., Futaš, P., Baricová, D. (2011). The influence of Ni and Cr-content on mechanical properties of Hadfield´s steel. In 20th Anniversary International Conference on Metallurgy and Materials. Metal 2011, 18-20.05.2011 (pp.1-6). Brno, Czech Republic.

[6]   Dastur, Y.N. & Leslie, W.C. (1981). Mechanism of work hardening in Hadfield manganese steel. *Metallurgical Transactions A*. 12A, 749-759.

[7]   Austenitic Manganese Steels. (June 2021). Retrieved August 13, 2021, from http://www.keytometals.com/ Articles/Art69.htm.

[8]   Stradomski, Z. (2010). *The role of microstructure in the wear behaviour of abrasion-resistant cast steels*. Częstochowa: Wyd. Politechniki Częstochowskiej. ISBN: 978-83-7193-468-1. (in Polish).

[9]   Kniaginin, G. (1977). *Cast steel. Metallurgy and founding*. Katowice: Wyd. Śląsk. (in Polish).

[10] Varela, L.B., Tressia, G., Masoumi, M., Bortoleto, E.M., Regattieri, C. & Sinatora, A. (2021). Roller crushers in iron mining, how does the degradation of Hadfield steel components occur. *Engineering Failure Analysis.* 122, 1-18.

[11] Głownia, J. (2002). *Alloy steel castings – applications*. Kraków: Wyd. FotoBit. ISBN: 83-917129-1-5. (in Polish).

[12] Kosturek, R., Maranda, A., Senderowski, C. & Zasada, D. (2016). Research into the application of explosive welding of metal sheets with Hadfield's steel (Mangalloy). *High-Energetic Materials*. 8, 91-102.

[13] White, C.H. & Honeycombe, R.W.K. (1962). Structural changes during the deformation of high purity iron-manganese-carbon alloys. *Journal Iron and Steel Institute.* 200, 457-466.

[14] Subramanyam, D.K., Swansiger, A.E., Avery, H.S. (1990). *Austenitic manganese steels* ASM Metals Handbook 1. Properties and Selections: Irons, Steels and High - Performance Alloys. (pp. 822-840). ASM International. ISBN: 978-1-62708-161-0.

[15] Quan Shan, Ru Ge, Zulai Li, Zaifeng Zhou, Yehua Jiang, Yun-Soo Lee, & Hong Wu. (2021). Wear properties of high-manganese steel strengthened with nano-sized V_2C precipitates. *Wear*. 482-483, 203922.

[16] Jia-li Cao, Ai-min Zhao, Ji-xiong Liu, Jian-guo He, & Ran Ding. (2014). Effect of Nb on microstructure and mechanical properties in non-magnetic high manganese steel. *Journal of Iron and Steel Research International*. 21(6), 600-605.

[17] Atasoy, O.A., Ozbaysal, K. & Inal, O.T. (1989). Precipitation of vanadium carbides in 0.8% C-13% Mn-1% V austenitic steel. *Journal of Materials Science*. 24, 1393-1398.

[18] Iglesiasa, C., Solórzanob, G. & Schulza, B. (2009). Effect of low nitrogen content on work hardening and microstructural evolution in Hadfield steel. *Materials Characterization*. 60(9), 971- 979.

[19] Mahlami, C.S., Pan, X. (2017). *Mechanical properties and microstructure evaluation of high manganese steel alloyed with vanadium*. Retrieved August 10, 2021, from https://doi.org/10.1063/1.4990236

[20] Delgado, F., Rodríguez, S.A., Coronado, J.J. (2019). Effect of chemical composition and shot peening treatment on Hadfield steel swing hammers exposed to impact wear.

International Tribology Council The 10th International Conference BALTTRIB'2019, 14–16 November 2019, (pp. 87-93). Kaunas, Lithuania: Vytautas Magnus University Agriculture Academy.

[21] Sant, S.B., & Smith, R.W. (1987). A study in the work-hardening behaviour of austenitic manganese steels. *Journal of Materials Science*. 22, 1808-1814.

[22] Adler, P.H., Olson, G.B. & Owen, W.S. (1986). Strain hardening of Hadfield manganese steel. *Metallurgical Transactions A*. 17a, 1725-1737.

[23] Malkiewicz, T. (1978). *Metallurgy of iron alloys*. Warszawa: Wyd. PWN. (in Polish).

[24] Ashok Kumar Srivastava, Karabi Das. (2008). Microstructural characterization of Hadfield austenitic manganese steel. *Journal of Materials Science*. 43(16), 5654-5658.

[25] Bolanowski, K. (2013). The influence of the hardness of the surface layer on the abrasion resistance of Hadfield steel. *Problemy Eksploatacji*. 1, 127-139.